# DEGRADANT CHARACTERIZATION REPORT

| | | | |
|---|---|---|---|
| **Document No:** | RC-035 | **Page:** | 1 of 27 |
| **Project Number:** | 8106 | **Report No:** | LD1966 |
| **Name:** | Structural Characterization of CC-00277 (Degradant) | | |

| REPORT PREPARED BY | | | |
|---|---|---|---|
| **Name** | **Department** | **Signature** | **Date** |
| [redacted] | AMRI-Bothell Research Center | [redacted] | 18 Sept 12 |

| REPORT APPROVED BY | | | |
|---|---|---|---|
| **Name** | **Department** | **Signature** | **Date** |
| [redacted] | AMRI-Bothell Research Center | [redacted] | 9-18-12 |
| | The Coca-Cola Company | | 9/25/12 |

## 1.0 Abstract


A degradant named CC-00277 was formed upon heating an acidic aqueous solution of CC-00276 and isolated from this solution. Spectrometric analysis revealed that the structure of this impurity is 13-[(2-*O*-6-deoxy-β-D-glucopyranosyl-3-*O*-β-D-glucopyranosyl-β-D-glucopyranosyl)oxy] *ent*-kaur-15-en-19-oic acid-[(2-*O* -β-D-xylopyranosyl -3-*O*-β-D-glucopyranosyl-β-D-glucopyranosyl) ester]. Evaluation of the data led to the conclusion that this degradant has an unsaturation at C-15 rather than C-16 as found in CC-00276 (Ref. 6.2).


## 2.0 Background

CC-00276 was degraded using the stress conditions described below which generated a number of major degradants one of which was subsequently identified as CC-00277. In order to identify CC-00277, it was isolated through a series of liquid chromatographic (LC) steps and then characterized by multiple nuclear magnetic resonance spectrometric (NMR) and mass spectrometric (MS) analyses.

## 3.0 Materials and Methods

Unless otherwise noted, all work was conducted at AMRI, Bothell Research Center, Bothell, Washington.

3.1 CC-00276. A sample of CC-00276, Lot VSPC-2973-6B, was obtained from Pure Circle, Malaysia.

3.2 LC-MS. Mass spectrometry was carried out on a Sciex API2000 triple quadrupole mass spectrometer with a TurboIonSpray ionization source operating in negative ion mode. A Sedere Sedex 75 ELS detector was used operating at 50 °C and 3.5 bar. Analysis of the samples was performed using the following method: Column: Phenomenex Synergi Hydro RP, 4.6 x 250 mm, 4 µm (p/n 00G-4375-E0); Column Temp: 55 °C; Mobile Phase A: $H_2O$ (0.0284% $NH_4OAc$, 0.0116% HOAc); Mobile Phase B: Acetonitrile; Flow Rate: 1.0 mL/min; Injection volume: 50 µL. Detection was by UV (210 nm), ELSD, and MSD (+ESI *m/z* 200-1450).

Gradient:

| Time (min) | %A | %B |
|---|---|---|
| 0.0 | 75 | 25 |
| 8.5 | 75 | 25 |
| 10.0 | 71 | 29 |
| 16.5 | 70 | 30 |
| 18.5 | 66 | 34 |
| 24.5 | 66 | 34 |
| 26.5 | 48 | 52 |
| 29.0 | 48 | 52 |
| 31.0 | 30 | 70 |

| | | |
|---|---|---|
| 37.0 | 30 | 70 |
| 37.1 | 75 | 25 |
| 45.0 | 75 | 25 |

3.3 Isolation of CC-00277 by HPLC.
The HPLC method was used for the isolation is summarized below. Column: Gemini $C_{18}$ with guard column, 250 x 10 mm, 5 µm (p/n 00G-4435-N0); Column Temp: 25 °C; Mobile Phase A: $H_2O$; Mobile Phase B: Acetonitrile; Flow Rate: 5.0 mL/min; Injection volume: 150 µL prepared in $H_2O$. Detection was by UV (210 nm).

| Time (min) | %A | %B |
|---|---|---|
| 0.0 | 75 | 25 |
| 20.0 | 69 | 31 |
| 20.5 | 50 | 50 |
| 25.0 | 40 | 60 |
| 25.1 | 75 | 25 |
| 30.0 | 75 | 25 |

3.4 MS and MS/MS. MS and MS/MS data were generated with a Waters Premier QTof mass spectrometer equipped with an electrospray ionization source. Samples were diluted with $H_2O$:acetonitrile (1:1) containing 0.1% formic acid and introduced via infusion using the onboard syringe pump. The samples were diluted to yield good s/n which occurred at an approximate concentration of 0.01 mg/mL.

3.5 NMR. The sample was prepared in pyridine-$d_5$ and NMR data were acquired on a Bruker Avance 500 MHz instrument with a 5 mm inverse detection probe. The spectrum was referenced to the residual solvent signal ($\delta_H$ 8.71, $\delta_C$ 149.9 for pyridine-$d_5$).

3.6 Degradation of CC-00276. A 0.1 M phosphoric acid solution was made and adjusted to pH 2.0 with concentrated ammonium hydroxide. Ten milligram of CC-00276 was added to 10 mL of phosphoric acid solution. The solution was placed on a heat block at 80 °C for 24 hours. A sample of the degradation mixture was analyzed using the LC-MS method described in Section 3.2.

4.0 Results and Discussion

4.1 Isolation and Purification. Isolation of CC-00277 was performed using CC-00276 degradation mixture that was prepared as described in Section 3.6. This material was analyzed by LC-MS using the LC-MS method (Section 3.2) and the results are given in Figure 1. The CC-00276 was observed at 11.52 min in the UV (210 nm) chromatogram. The mass spectrum for the CC-00276 peak provided the expected $[M-H]^-$ ion at *m/z* 1289.7. The CC-00277 peak was observed to elute at 13.36 min in the UV chromatogram and showed an $[M-H]^-$ ion at *m/z* 1289.7. This indicated that CC-00277 indicated that it is an isomer of CC-00276 which

together with the retention time suggested that it may be CC-00277. HPLC purification was performed using HPLC Method as describe in Section 3.3 and the peak eluting at 13.19 min was collected over several injections and dried by rotary evaporation under reduced pressure (Figure 2).

4.2 Mass Spectrometry. The results of an LC-MS analysis of the isolated degradant peak are shown in Figure 3 and confirmed that it corresponded to CC-00277. A single peak was observed in the TIC, UV and ELS chromatograms. The mass spectrum of the isolated degradant showed an $[M-H]^-$ ion at *m/z* 1290.4.

The ESI+ TOF mass spectrum acquired by infusing a sample of CC-00277 showed $[M+H]^+$ and $[M+Na]^+$ ions at *m/z* 1291.5439 and 1313.5254, respectively (Figure 4). The mass of the $[M+H]^+$ ion was in good agreement with the molecular formula $C_{56}H_{90}O_{33}$ (calcd for $C_{56}H_{91}O_{33}$: 1291.5443, error: -0.3 ppm) for CC-00277 (Figure 5). The ESI- mass spectrum provided $[M-H]^-$ and $[M+HCOOH-H]^-$ ions at *m/z* 1289.5304 and 1335.5366, respectively (Figure 6). As above, the mass of the $[M-H]^-$ ion was in good agreement with the molecular formula $C_{56}H_{90}O_{33}$ (calcd for $C_{56}H_{89}O_{33}$: 1289.5286, error: 1.4 ppm) for CC-00277 (Figure 7). The +ESI and -ESI data indicated that CC-00277 has a nominal mass of 1290 Daltons with the molecular formula, $C_{56}H_{90}O_{33}$. This confirms that CC-00277 is an isomer of CC-00276.
The +ESI TOF MS/MS spectrum of CC-00277, fragmenting on the $[M+H]^+$ ion at *m/z* 1291 is shown in Figure 8 and provided fragment ions corresponding to the sequential loss of glucose residues at *m/z* 1129.4908, 967.4387, 805.3853, and 643.3348. A fragment ion was also observed at *m/z* 973.3253 corresponding to six glucose residues. This ion underwent sequential loss glucose to yield fragment ions at *m/z* 811.2714, 649.2180, 487.1656, and 325.1151. This was identical to the fragmentation pattern observed for CC-00276.

The -ESI TOF MS/MS spectrum of CC-00277, fragmenting on the $[M-H]^-$ ion at *m/z* 1289 indicated that the most abundant and readily formed ion is present at *m/z* 803.3706 and corresponds to the loss of three glucose residues (Figure 9). Since this fragmentation likely results at C-19 it suggested that the glycoside at C-19 is composed of three glucose residues as found in CC-00276.

4.3 NMR Spectrometry.
A series of NMR experiments including $^1$H NMR (Figure 10), $^1$H-$^1$H COSY (Figure 11), HSQC (Figure 12), and HMBC (Figure 13) were performed to allow the assignment of CC-00277.

An HMBC correlation from the methyl protons at $\delta_H$ 1.35 ppm to the carbonyl at $\delta_C$ 176.7 allowed assignment of one of the tertiary methyl groups (C-18) as well as C-19 and provided a starting point for assignment of the rest of the aglycone. Additional HMBC correlations from the methyl protons (H-18) to carbons at $\delta_C$ 38.0, 44.0, and 56.9 allowed assignment of C3 to C5 in comparison with the data for CC-00276 (Ref 6.2). The $^1$H chemical shifts for C-3 ($\delta_H$ 1.03 and 2.33) and C-

5 ($\delta_H$ 1.05) were assigned using the HSQC data. A COSY correlation between one of the H-3 protons ($\delta_H$ 1.03) and a proton at $\delta_H$ 1.36 allowed assignment of one of the H-2 protons which in turn showed a correlation with a proton at $\delta_H$ 0.77 which was assigned to C-1. The remaining $^1H$ and $^{13}C$ chemical shifts for C-1 and C-2 were then assigned on the basis of additional COSY and HSQC correlations and are summarized in Table 1.

A second tertiary methyl singlet, observed at $\delta_H$ 1.33 showed HMBC correlations to C-1 and C-5 and was assigned as C-20. The methyl protons showed additional HMBC correlations to a quaternary carbon ($\delta_C$ 39.6) and a methine ($\delta_H$ 0.83, $\delta_C$ 47.0) which were assigned as C-10 and C-9, respectively. COSY correlations between H-5 ($\delta_H$ 1.05) and protons at $\delta_H$ 2.21 and 2.31 then allowed assignment of the H-6 protons which in turn showed correlations to protons at $\delta_H$ 1.49 and 1.89 which were assigned to C-7. The $^{13}C$ chemical shifts for C-6 ($\delta_C$ 21.8) and C-7 ($\delta_C$ 40.0) were then determined from the HSQC data.

COSY correlations between H-9 ($\delta_H$ 0.83) and protons at $\delta_H$ 1.56 and 1.67 allowed assignment of the H-11 protons which in turn showed COSY correlations to protons at $\delta_H$ 1.84 and 2.36 which were assigned as the H-12 protons. The HSQC data was then used to assign C-11 ($\delta_C$ 20.9) and C-12 ($\delta_C$ 29.9).

A third tertiary methyl group was observed in the $^1H$ NMR spectrum of CC-00277 at $\delta_H$ 1.89 which was not observed for CC-00276 and suggested a change in the aglycone for this impurity. This methyl group showed HMBC correlations to carbons at $\delta_C$ 89.6, 134.3, and 144.4. HMBC correlations were also observed between the methylene protons at C-12 ($\delta_H$ 1.84 and 2.36) and carbons at $\delta_C$ 89.6 and 144.4 allowing them to be assigned as C-13 and C-16, respectively. The olefinic proton observed as a singlet at $\delta_H$ 5.03 showed an HSQC correlation to the carbon at $\delta_C$ 134.3 which was assigned as C-15 and a methyl carbon at $\delta_C$ 12.7 which was assigned as C-17. An HMBC correlation was also observed between H-9 and the carbon at $\delta_C$ 144.4 confirming the assignment of C-15. An additional HMBC correlation between H-9 and an isolated methylene group ($\delta_H$ 2.17 and 2.69, $\delta_C$ 47.1) allowed the assignment of C-14. HMBC correlations between the H-14 protons and C-13, C-15, and C-16 confirmed the assignment of the methylene group at C-14.

Analysis of the NMR data indicated that CC-00277 has a rearrangement in the aglycone resulting in a shift in the unsaturation from C-16 to C-15. A summary of the $^1H$ and $^{13}C$ chemical shifts for the aglycone are found in Table 1 and a summary of the key HMBC and COSY correlations used to assign the aglycone region are provided in Figure 14.

An analysis of the HSQC data for CC-00277 confirmed the presence of 6 anomeric positions. Three of the anomeric protons were well resolved at $\delta_H$ 6.33 ($\delta_C$ 94.5), 5.81 ($\delta_C$ 103.8), and 5.33 ($\delta_C$ 103.9) in the $^1H$ NMR spectrum. The remaining three anomeric protons were observed at $\delta_H$ 5.47 ($\delta_C$ 95.7), 5.45 ($\delta_C$ 104.5), and 5.44 ($\delta_C$ 103.9) and were overlapped in the $^1H$ spectrum. The

anomeric proton observed at $\delta_H$ 6.33 showed an HMBC correlation to C-19 which indicated that it corresponds to the anomeric proton of $Glc_I$. Similarly, the anomeric proton observed at $\delta_H$ 5.47 showed an HMBC correlation to C-13 allowing it to be assigned as the anomeric proton of $Glc_{II}$.

The $Glc_I$ anomeric proton ($\delta_H$ 6.33) showed a COSY correlation to a proton at $\delta_H$ 4.51 which was assigned as $Glc_I$ H-2 and in turn showed a COSY correlation to a proton at $\delta_H$ 4.99 ($Glc_I$ H-3) which showed a correlation with a proton at $\delta_H$ 4.19 ($Glc_I$ H-4). Assignment of the $^{13}C$ chemical shifts for $Glc_I$ C-2 ($\delta_C$ 76.6), C-3 ($\delta_C$ 88.3), and C-4 ($\delta_C$ 69.6) was made using the HSQC data. An HMBC correlation between H-1 and a carbon at $\delta_C$ 78.1 allowed assignment of C-5 in comparison with the data for CC-00276 with H-5 ($\delta_H$ 4.10) then assigned from the HSQC data. The assignment at $Glc_I$ C-6 was made using the $^1H$ and HSQC data in comparison with the data for CC-00276.

Assignment of $Glc_{II}$ was carried out in a similar fashion. The $Glc_{II}$ anomeric proton ($\delta_H$ 5.47) showed a COSY correlation to a proton at $\delta_H$ 4.13 which was assigned as $Glc_{II}$ H-2 and in turn showed a COSY correlation to a proton at $\delta_H$ 4.89 ($Glc_{II}$ H-3) which showed an additional correlation with a proton at $\delta_H$ 4.04 ($Glc_{II}$ H-4) which showed a correlation to a proton at $\delta_H$ 3.90 ($Glc_{II}$ H-5). Assignment of the $^{13}C$ chemical shifts for $Glc_{II}$ C-2 ($\delta_C$ 81.1), C-3 ($\delta_C$ 87.6), C-4 ($\delta_C$ 70.0) and C-5 ($\delta_C$ 77.4) was then completed using the HSQC data. The assignment at $Glc_{II}$ C-6 was made using the $^1H$, COSY and HSQC data in comparison with the data for CC-00276.

Two of the remaining unassigned glucose moieties were assigned as substituents at C-2 and C-3 of $Glc_I$ on the basis of HMBC correlations. The anomeric proton observed at $\delta_H$ 5.81 showed an HMBC correlation to $Glc_I$ C-2 and was assigned as the anomeric proton of $Glc_V$. The anomeric proton observed at $\delta_H$ 5.33 showed an HMBC correlation to $Glc_I$ C-3 and was assigned as the anomeric proton of $Glc_{VI}$. The reciprocal HMBC correlations between $Glc_I$ H-2 and anomeric carbon of $Glc_V$ and between $Glc_I$ H-3 and the anomeric carbon of $Glc_{VI}$ were also observed. The assignments for C-2 through C-6 of $Glc_V$ and $Glc_{VI}$ were made using the $^1H$, COSY and HSQC data in comparison with the assignment of CC-00276.

Analysis of the data indicated that the C-19 glycoside found in CC-00277 is identical to that found in CC-00276. A summary of the $^1H$ and $^{13}C$ chemical shifts for the glycoside at C-19 are found in Table 2 and a summary of the key HMBC and COSY correlations used to assign the C-19 glycoside region are provided in Figure 15.

The two remaining unassigned sugar moieties were assigned as substituents at C-2 and C-3 of $Glc_{II}$ on the basis of HMBC correlations. The anomeric proton observed at $\delta_H$ 5.45 showed an HMBC correlation to $Glc_{II}$ C-2 and was assigned as the anomeric proton of $Glc_{III}$. The anomeric proton observed at $\delta_H$ 5.44 showed an HMBC correlation to $Glc_{II}$ C-3 and was assigned as the anomeric

proton of $Glc_{IV}$. The reciprocal HMBC correlation between $Glc_{II}$ H-2 and anomeric carbon of $Glc_{III}$ was observed as was the HMBC correlation between $Glc_{II}$ H-3 and the anomeric carbon of $Glc_{IV}$. The assignments for C-2 through C-6 of $Glc_{III}$ and $Glc_{IV}$ were made using the $^{1}H$, COSY and HSQC data in comparison with the assignment of CC-00276.

Analysis of the data indicated that the C-13 glycoside found in CC-00277 is identical to that found in CC-00276. A summary of the $^{1}H$ and $^{13}C$ chemical shifts for the glycoside at C-13 are found in Table 3 and a summary of the key HMBC and COSY correlations used to assign the C-13 glycoside region are provided in Figure 16. The structure of CC-00277 is shown in Figure 17.

4.4 Chromatography. When analyzed under the conditions of the LC/MS method described above, CC-00277 had a retention time of 13.2 min.

## 5.0 Conclusions

NMR and MS analyses of CC-00277 allowed a full assignment of its structure. The chemical name of CC-00278 is 13-[(2-*O*-6-deoxy-β-D-glucopyranosyl-3-*O*-β-D-glucopyranosyl-β-D-glucopyranosyl)oxy] *ent*-kaur-15-en-19-oic acid-[(2-*O*-β-D-xylopyranosyl -3-*O*-β-D-glucopyranosyl-β-D-glucopyranosyl) ester].

## 6.0 References


6.1 AMRI-Bothell Research Center Notebook # 833 pp. 1, 17, 18, and 38-47.

6.2 RC-032 "Structural Characterization of CC-00276"

## 7.0 Appendices and Attachments

### 7.1 Figure 1. LC-MS analysis of CC-00276 degradant mixture showing TIC (**A**), mass spectrum of the CC-00276 peak at 11.52 min (**B**), mass spectrum of the degradant peak at 13.36 min (**C**) and ELS chromatogram (**D**).

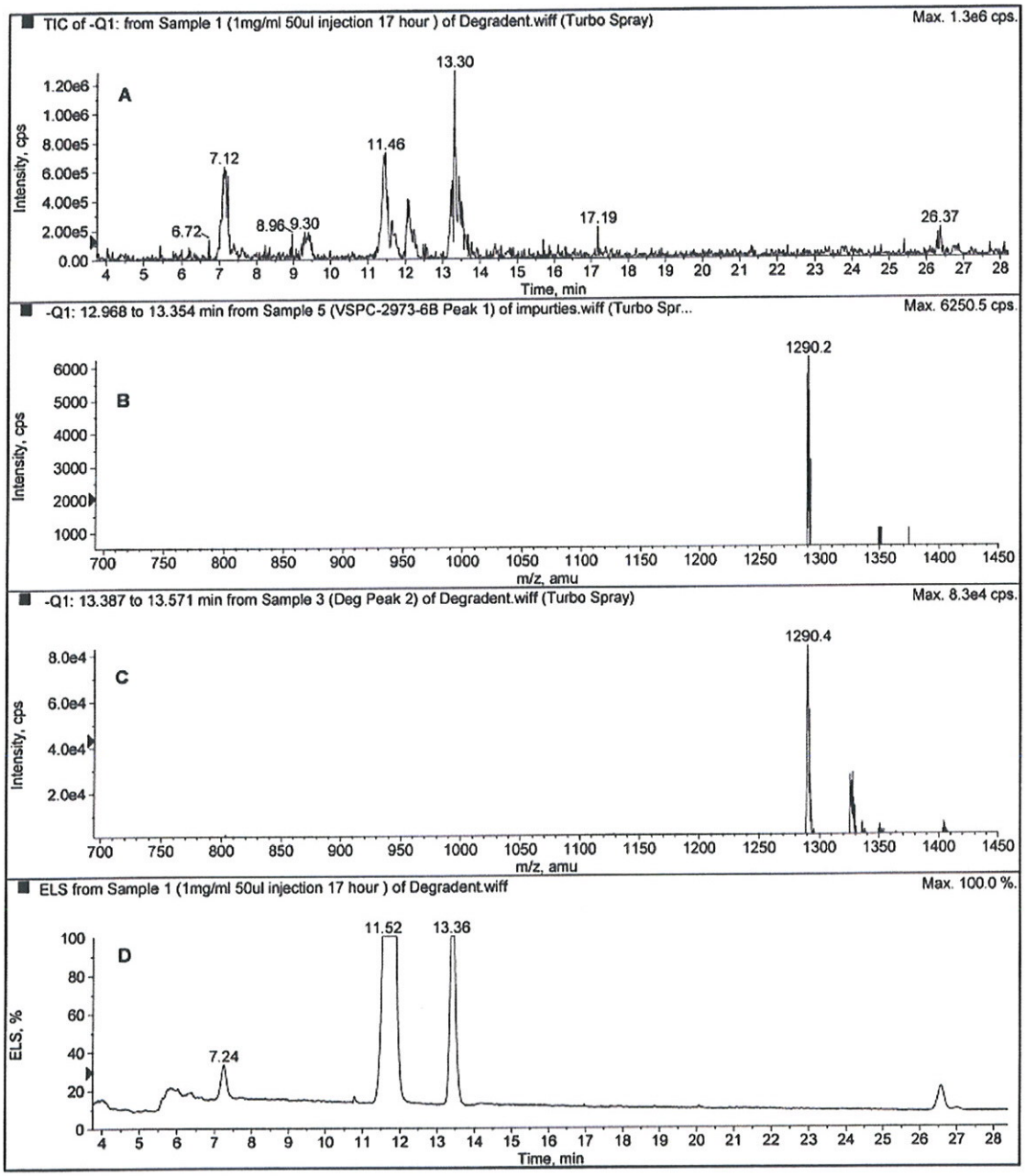

7.2 Figure 2. Representative HPLC UV (210 nm) chromatogram for the crude degradant fraction.

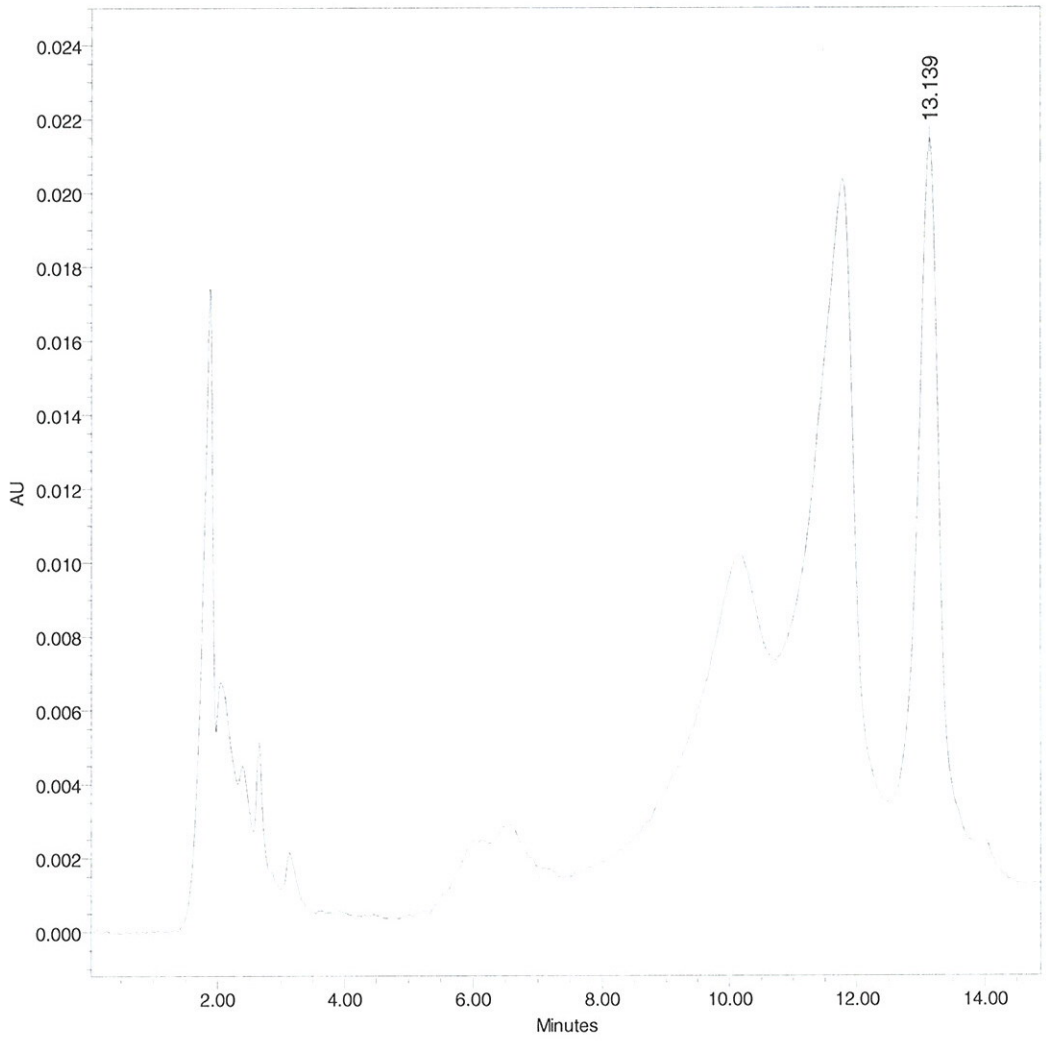

7.3 Figure 3. LC-MS analysis of isolated sample of the degradant showing TIC (**A**), mass spectrum of the degradant peak at 13.3 min (**B**), ELS chromatogram (**C**) and UV (210 nm) chromatogram (**D**).

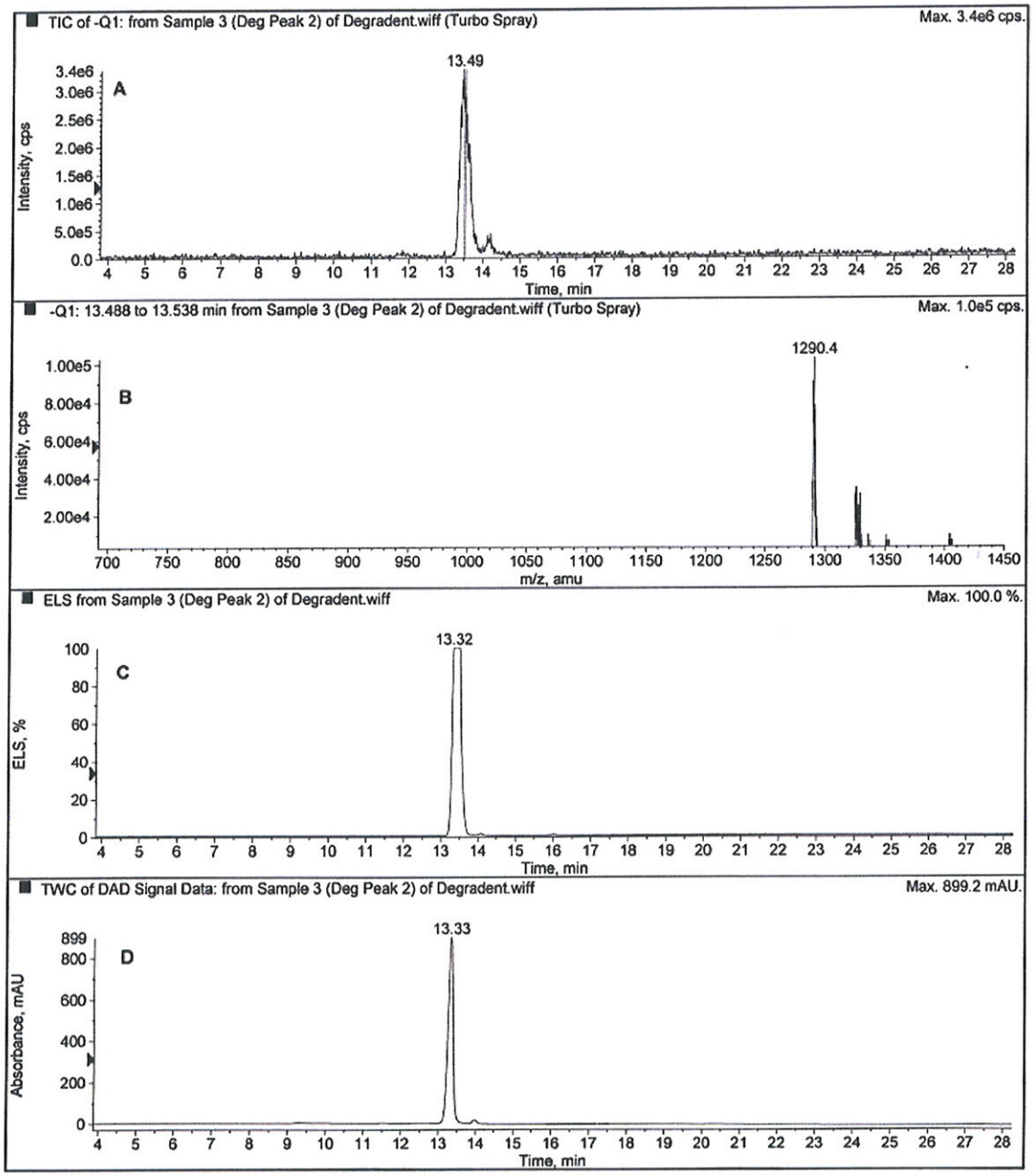

7.4 Figure 4. ESI+ TOF mass spectrum of CC-00277.

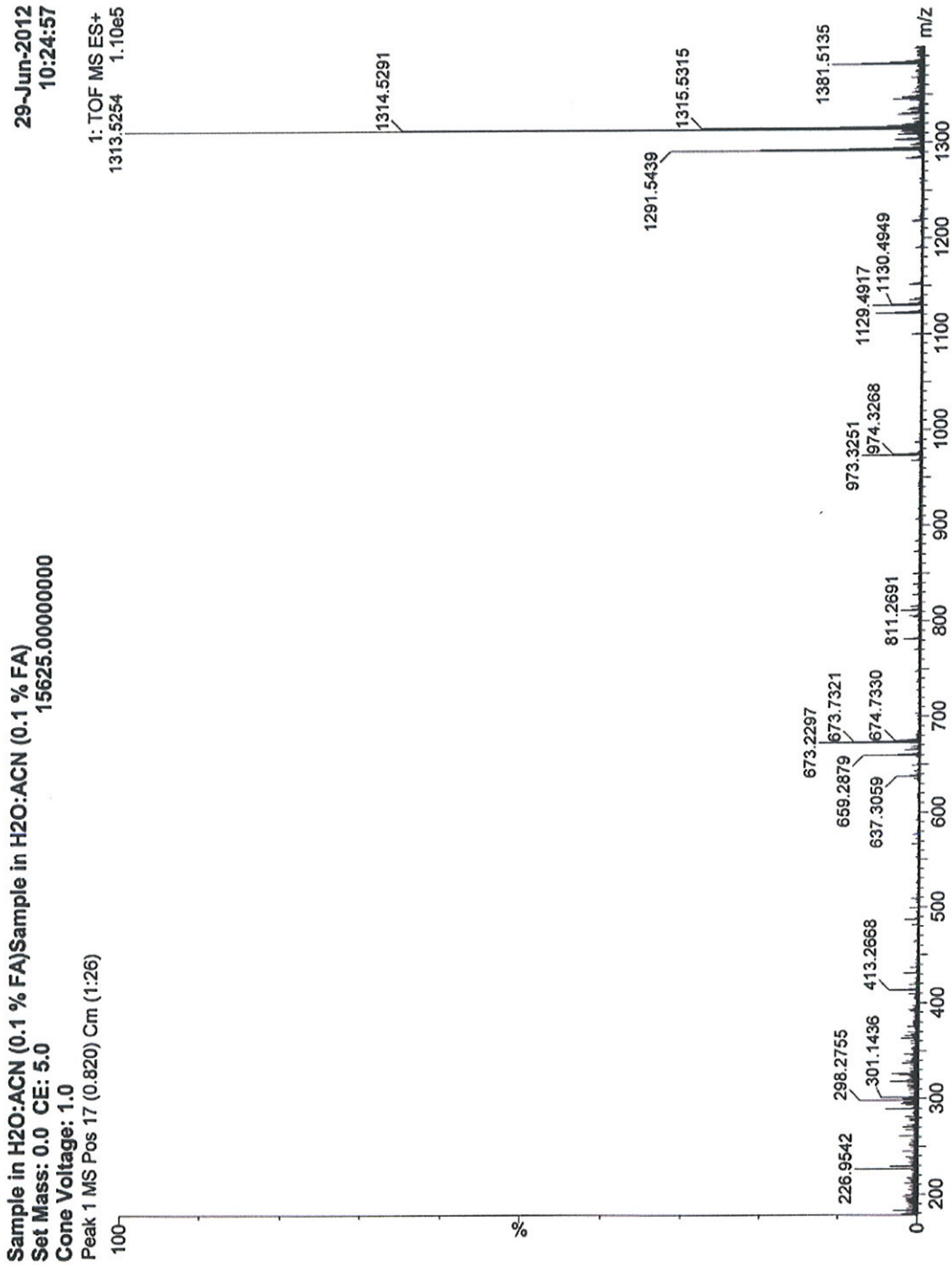

7.5 Figure 5. Accurate mass analysis of the $[M+H]^+$ ion of CC-00277.

**Single Mass Analysis**
Tolerance = 5.0 PPM / DBE: min = -1.5, max = 50.0
Selected filters: None

Monoisotopic Mass, Even Electron Ions
54 formula(e) evaluated with 1 results within limits (up to 50 closest results for each mass)
Elements Used:
C: 0-60 H: 0-95 O: 0-35

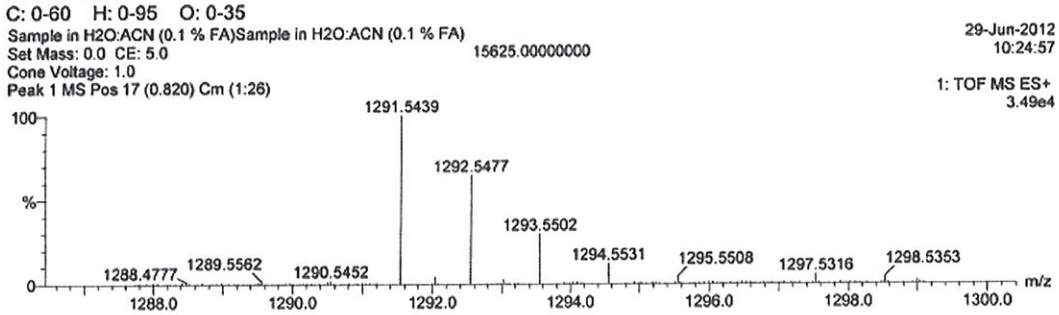


| | | | | | | |
|---|---|---|---|---|---|---|
| Minimum: | | | | -1.5 | | |
| Maximum: | | 3.0 | 5.0 | 50.0 | | |
| Mass | Calc. Mass | mDa | PPM | DBE | i-FIT | Formula |
| 1291.5439 | 1291.5443 | -0.4 | -0.3 | 11.5 | 23.3 | C56 H91 O33 |

7.6 Figure 6. ESI- TOF mass spectrum of CC-00277.

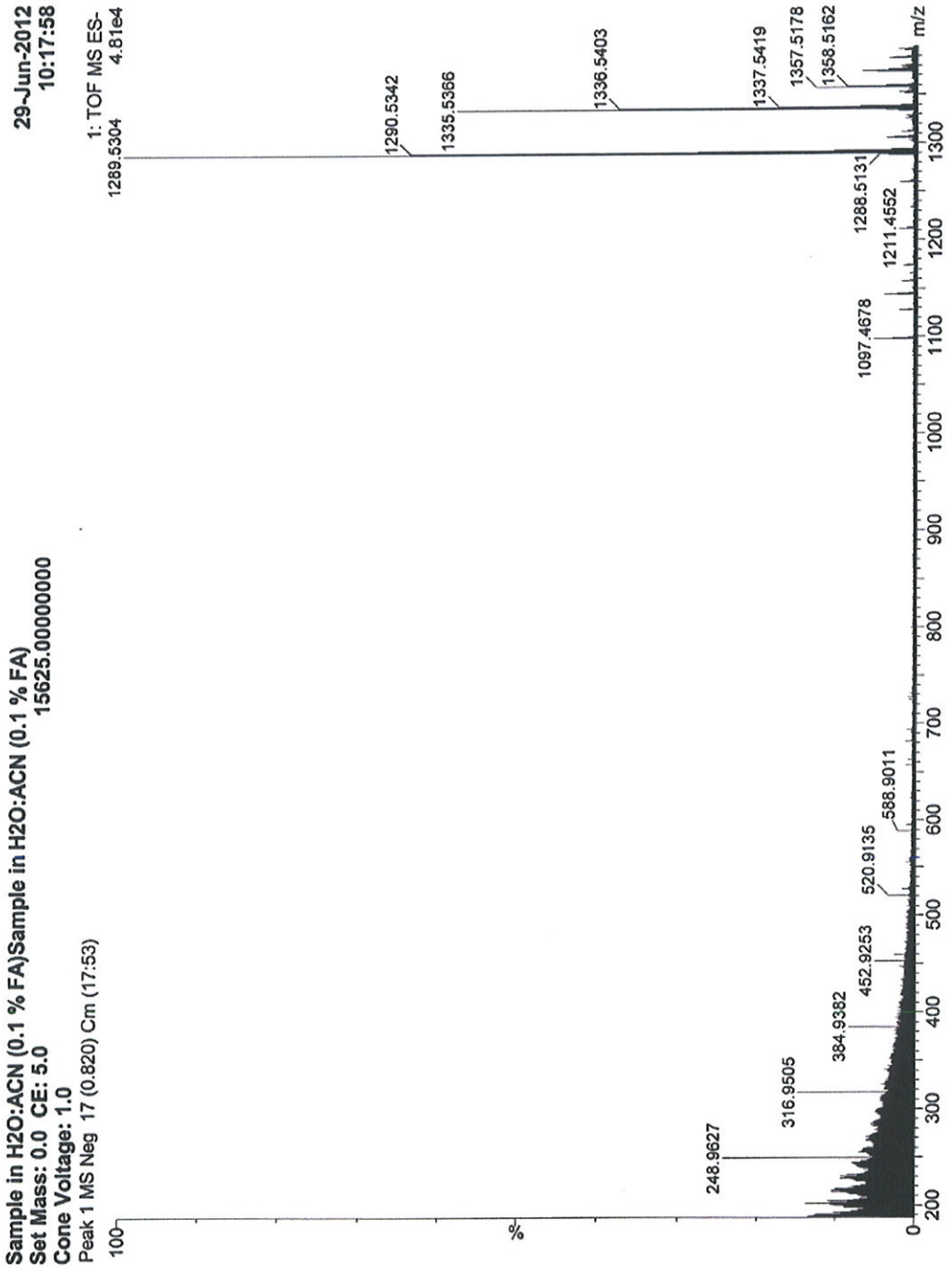

7.7 Figure 7. Accurate mass analysis of the $[M-H]^-$ ion of CC-00277.

**Single Mass Analysis**
Tolerance = 5.0 PPM / DBE: min = -1.5, max = 50.0
Selected filters: None

Monoisotopic Mass, Even Electron Ions
54 formula(e) evaluated with 1 results within limits (up to 50 closest results for each mass)
Elements Used:
C: 0-60 H: 0-95 O: 0-35

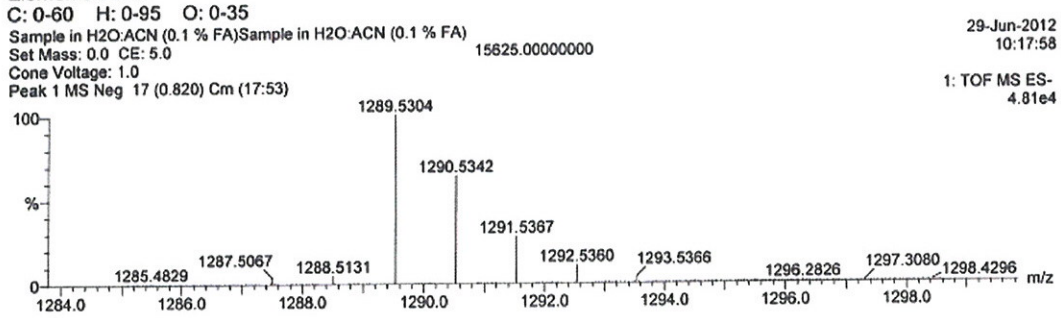


| | | | | | | |
|---|---|---|---|---|---|---|
| Minimum: | | | | -1.5 | | |
| Maximum: | | 3.0 | 5.0 | 50.0 | | |
| Mass | Calc. Mass | mDa | PPM | DBE | i-FIT | Formula |
| 1289.5304 | 1289.5286 | 1.8 | 1.4 | 12.5 | 4.9 | C56 H89 O33 |

7.8 Figure 8. ESI+ TOF MS/MS analysis of CC-00277 selecting the $[M+H]^+$ ion at *m/z* 1291 for fragmentation.

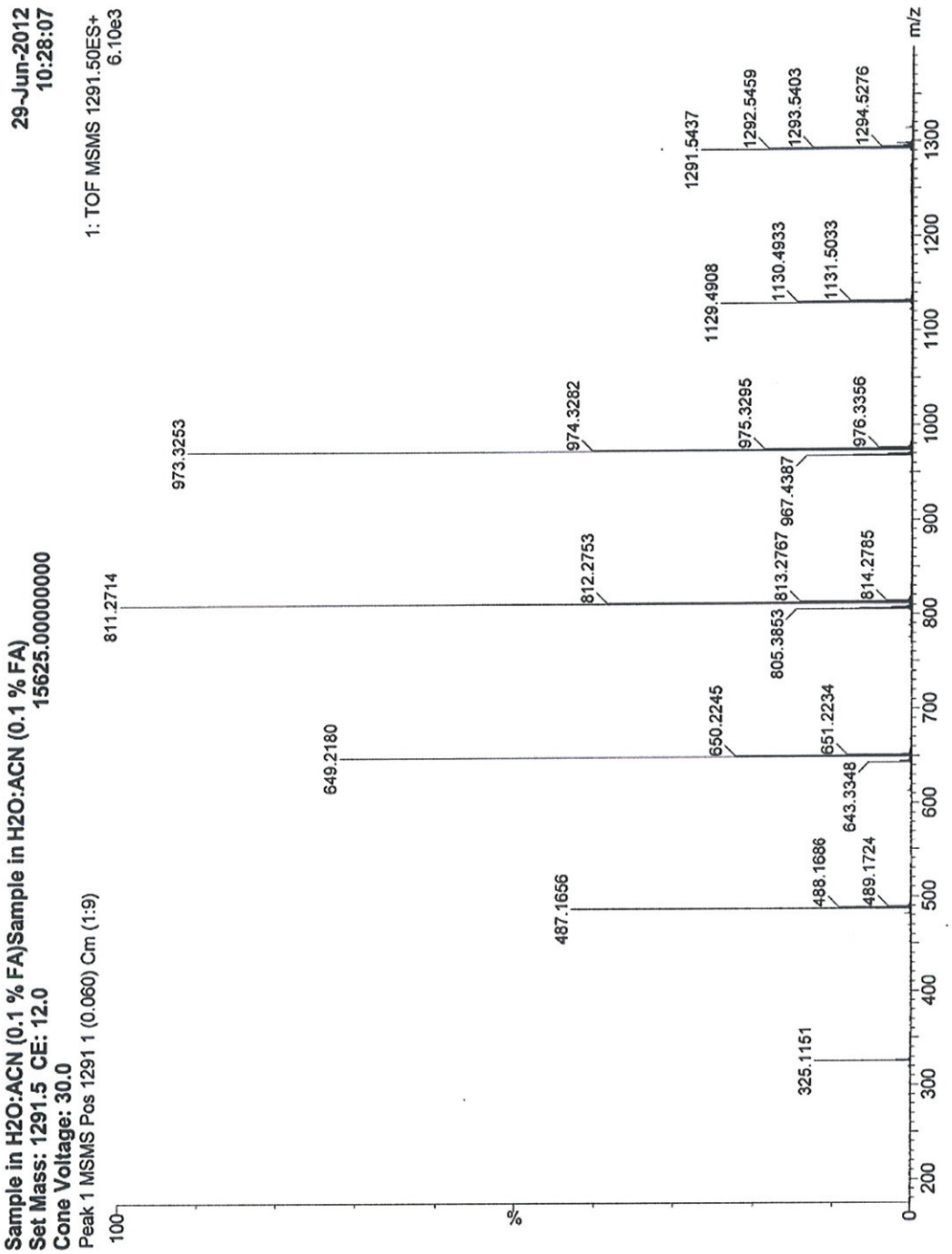

7.9 Figure 9. ESI- TOF MS/MS analysis of CC-00277 selecting the $[M-H]^-$ ion at *m/z* 1289 for fragmentation

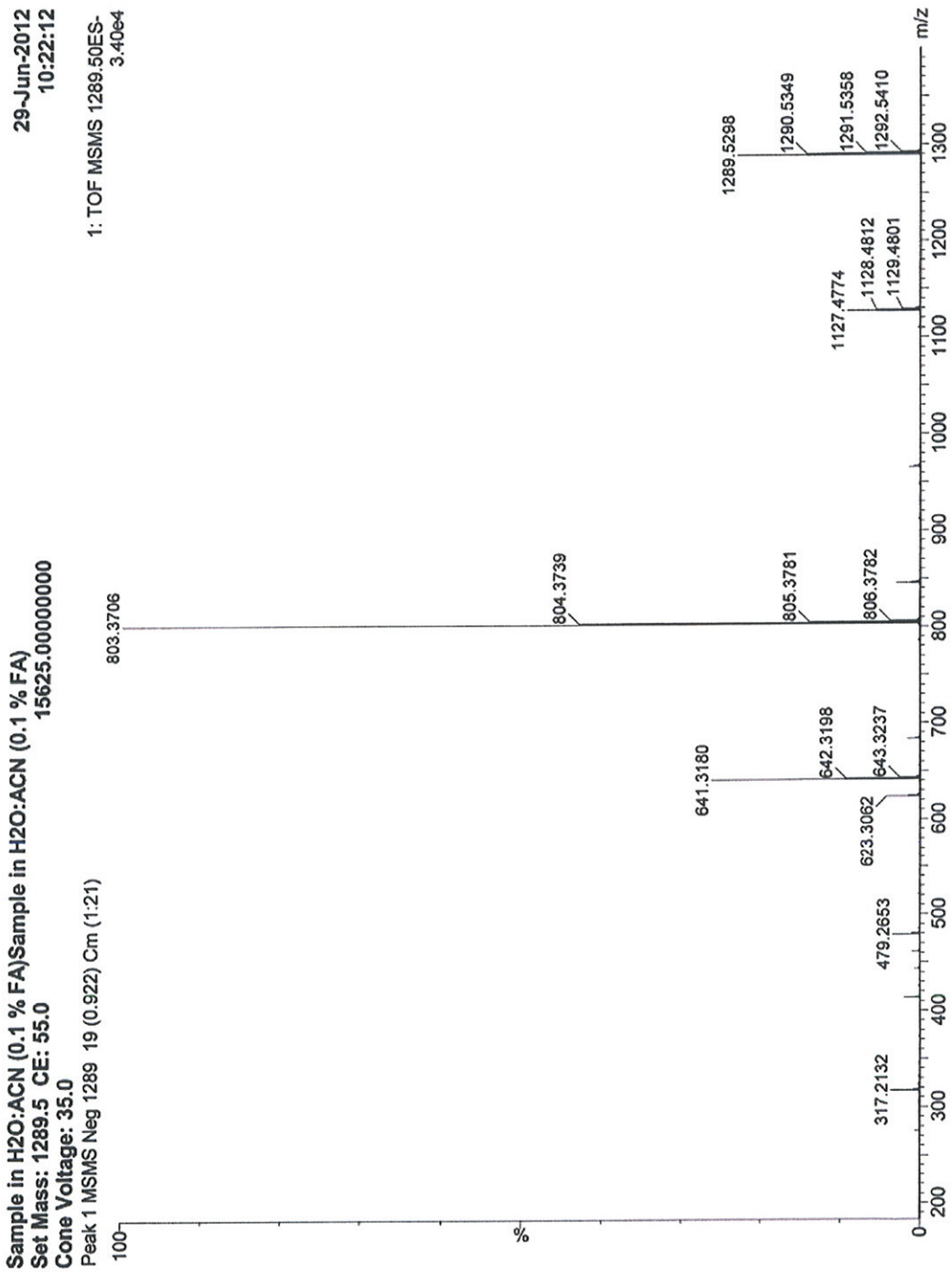

7.10 Figure 10. $^{1}H$ NMR (500 MHz, pyridine-$d_5$) of CC-00277.

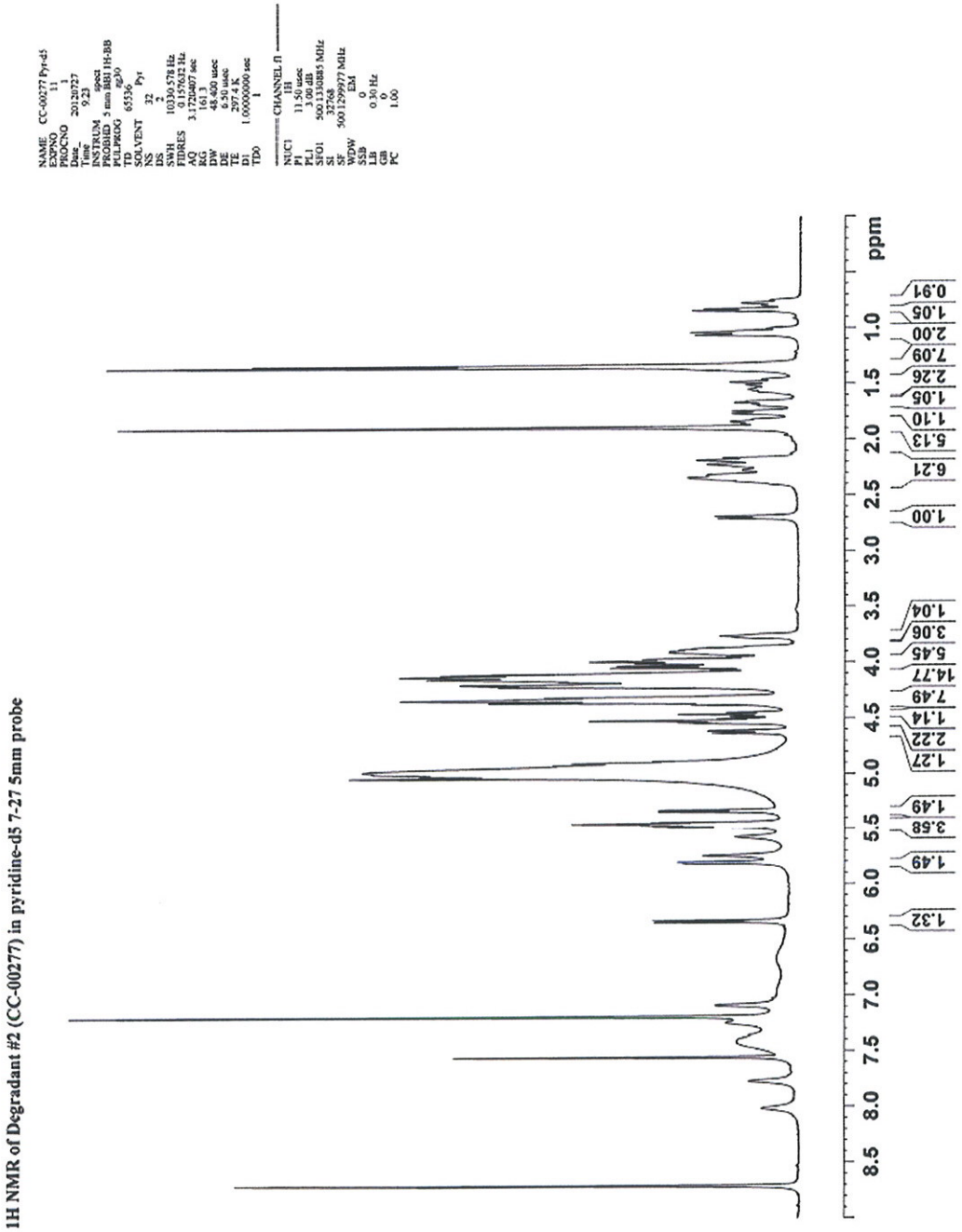

7.11 Figure 11. $^{1}H$-$^{1}H$ COSY Spectrum (500 MHz, pyridine-$d_5$) of CC-00277.

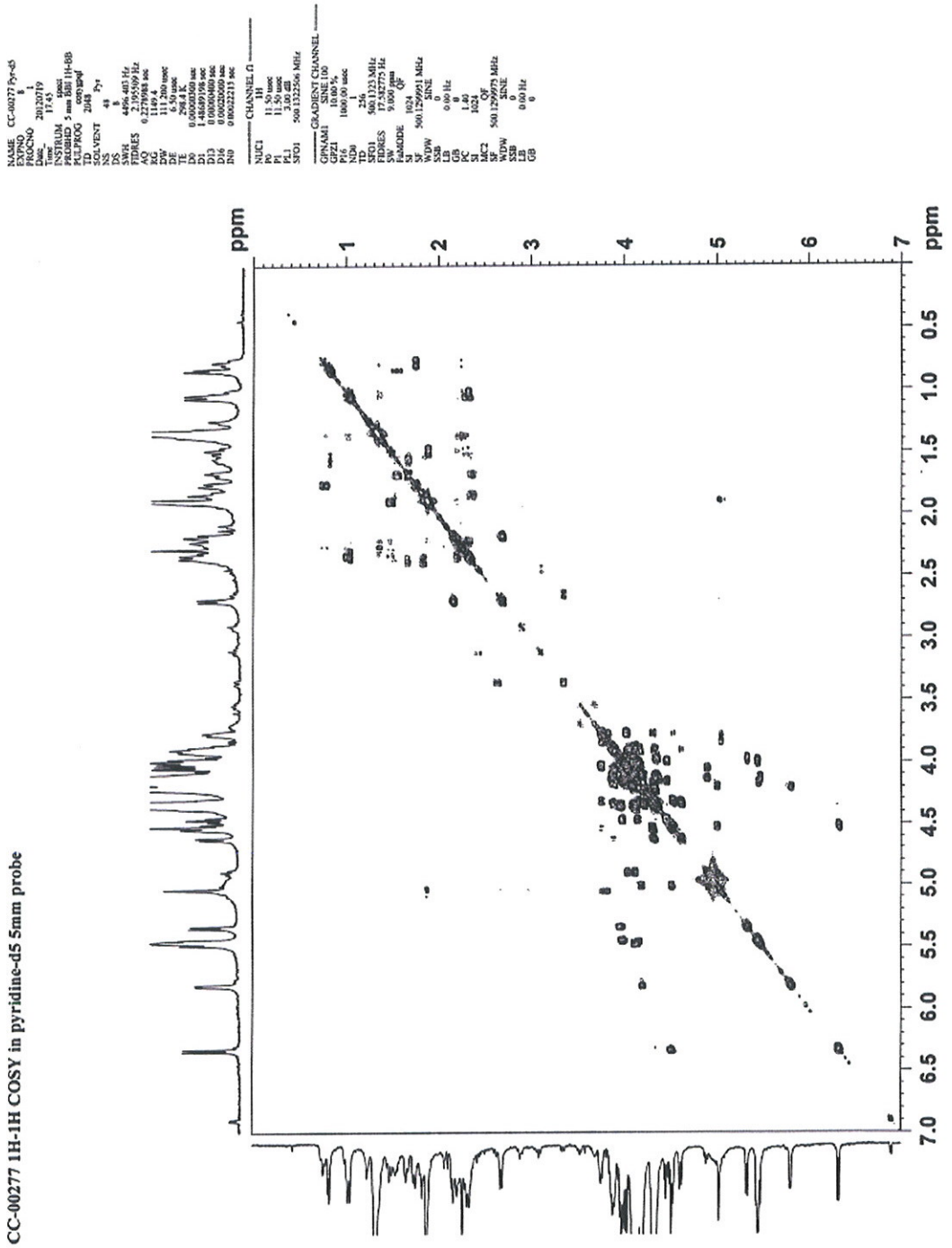

7.12 Figure 12. HSQC Spectrum (500 MHz, pyridine-$d_5$) of CC-00277.

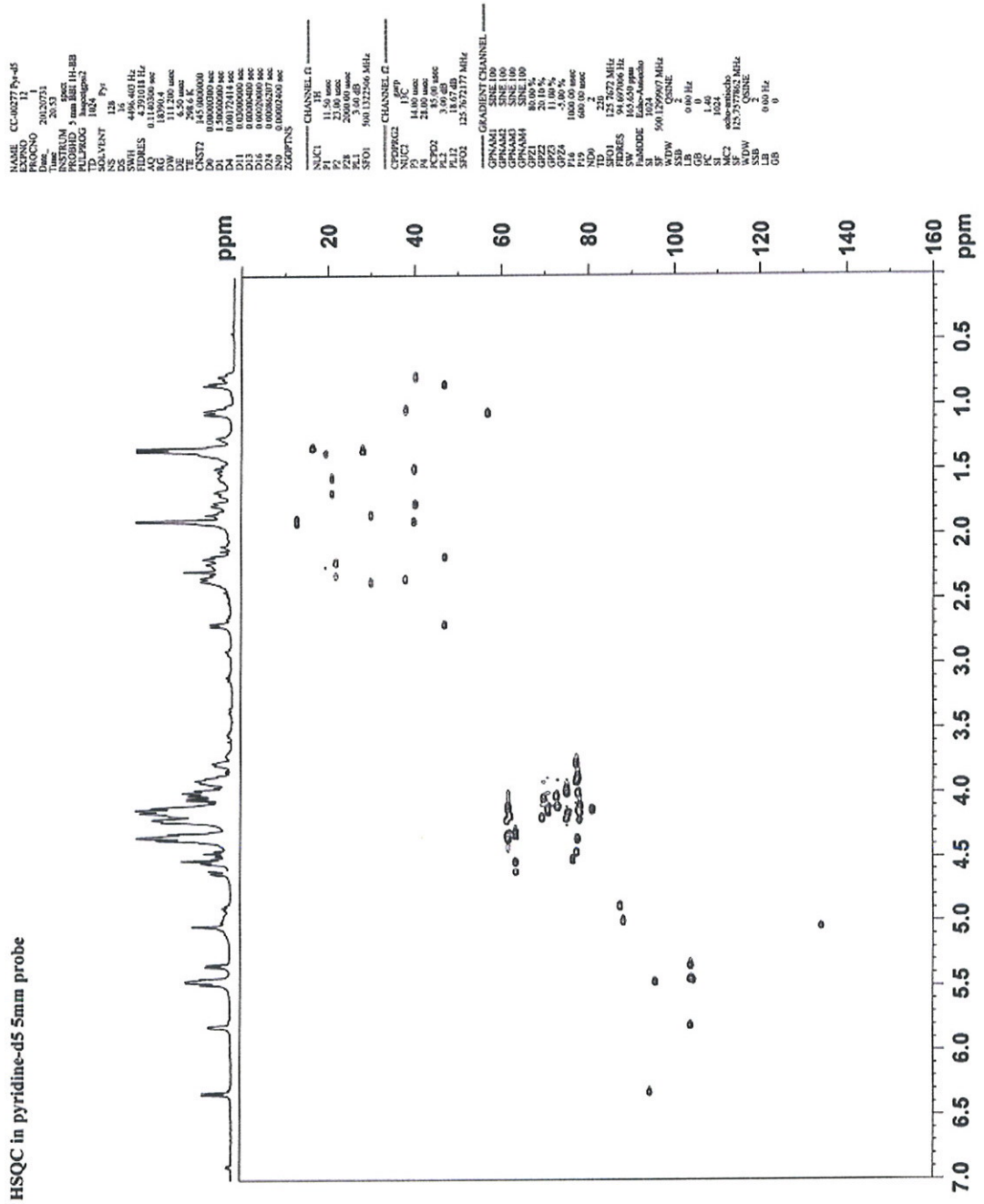

7.13 Figure 13. HMBC Spectrum (500 MHz, pyridine-$d_5$) of CC-00277.

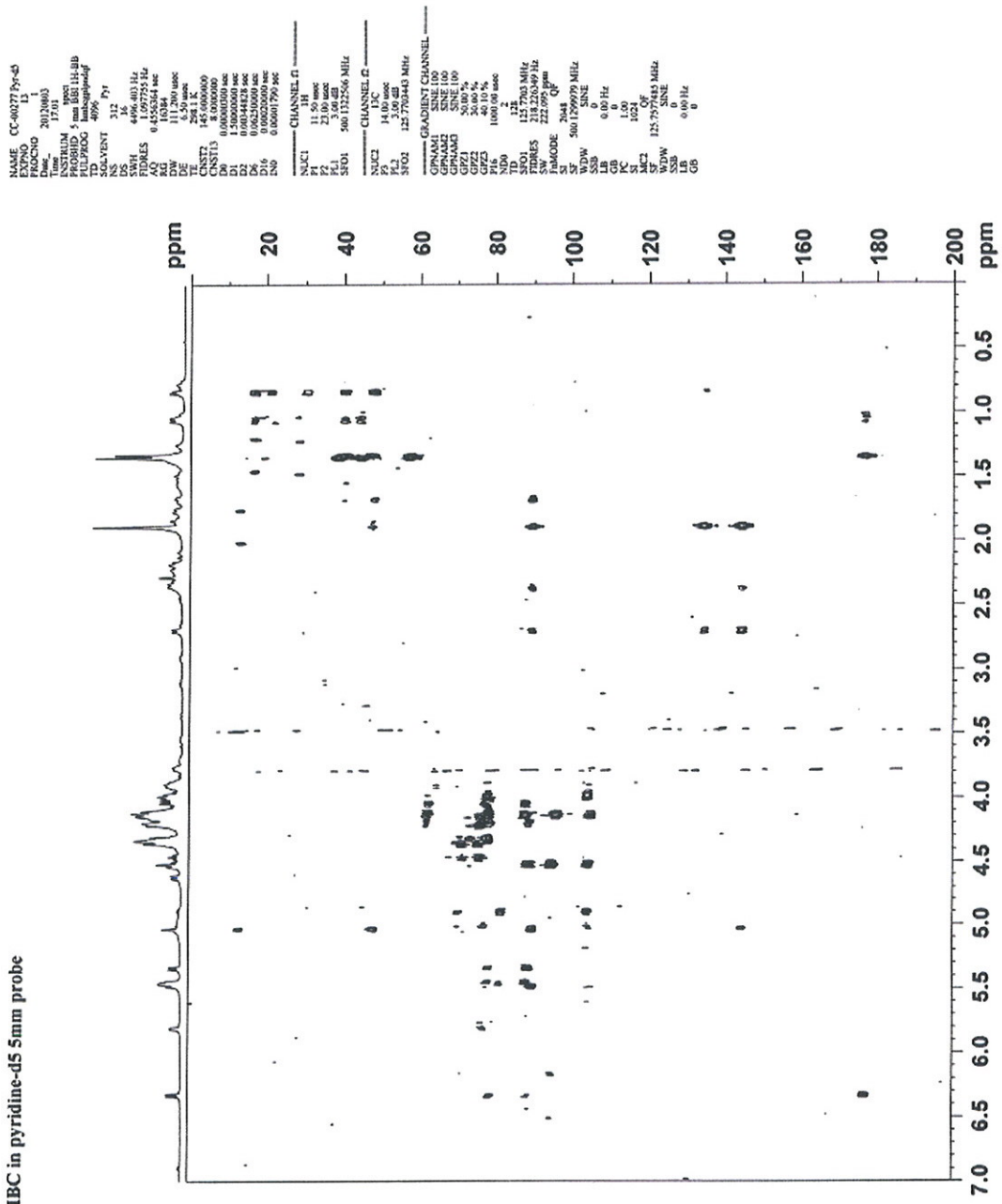

7.14 Figure 14. Summary of Key HMBC and COSY correlations used to assign the aglycone region of CC-00277.

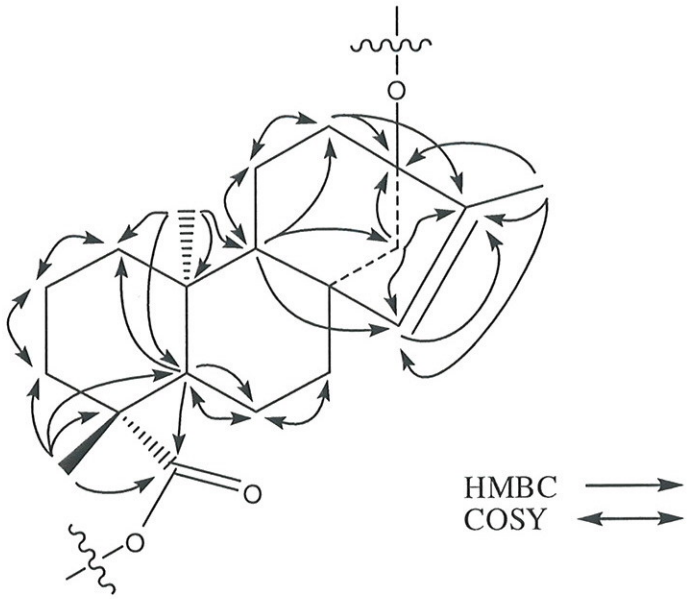

7.15 Figure 15. Summary of Key HMBC and COSY correlations used to assign the C-19 glycoside region of CC-00277.

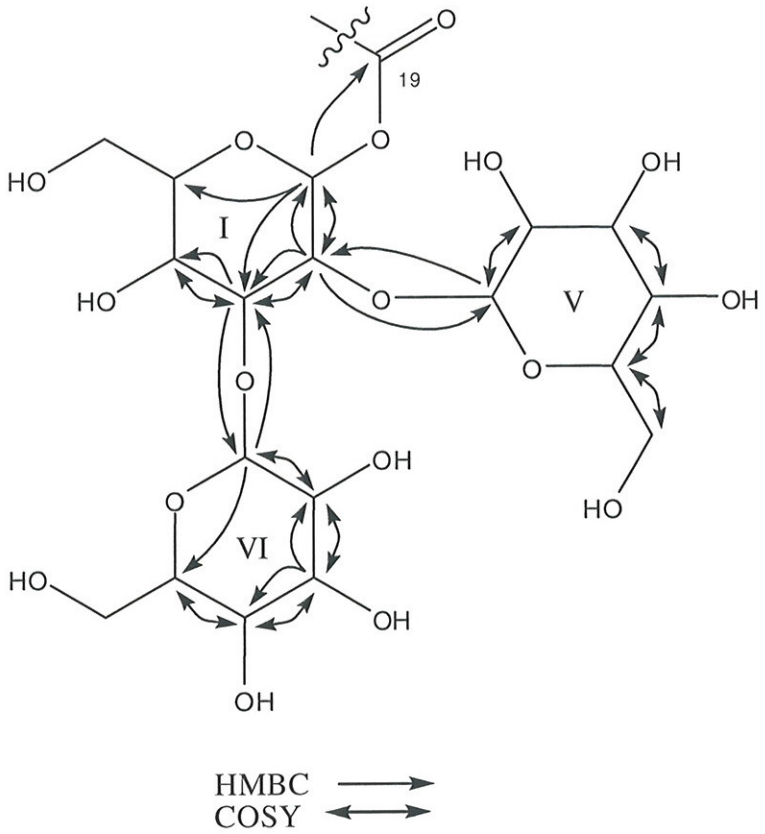

7.16 Figure 16. Summary of Key HMBC and COSY correlations used to assign the C-13 glycoside region of CC-00277.

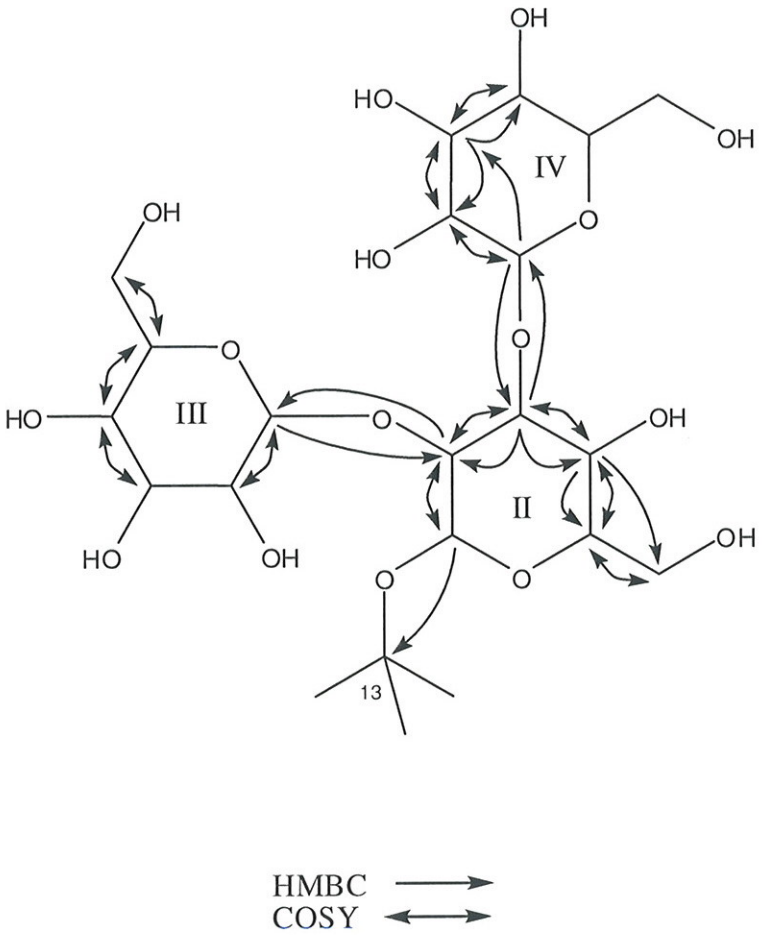

7.17 Figure 17. Structure of CC-00277.

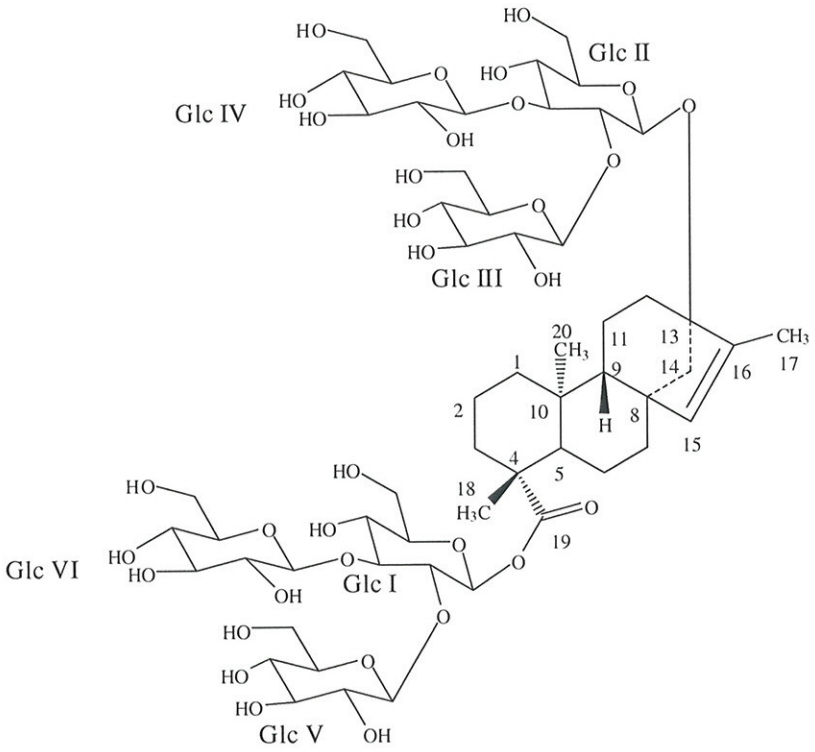


CC-00277

7.18 Table 1. $^{1}H$ and $^{13}C$ NMR (500 and 125 MHz, pyridine-$d_5$) Assignments of the CC-00277 aglycone.

| | CC-00277 | |
|---|---|---|
| Position | $^{13}C$ | $^{1}H$ |
| 1 | 40.2 | 0.77 t (12.8)<br>1.76 d (12.8) |
| 2 | 19.3 | 1.36 m<br>2.25 m |
| 3 | 38.0 | 1.03 m<br>2.33 m |
| 4 | 44.0 | --- |
| 5 | 56.9 | 1.05 d (12.7) |
| 6 | 21.8 | 2.21 m<br>2.31 m |
| 7 | 40.0 | 1.49 m<br>1.89 m |
| 8 | | --- |
| 9 | 47.0 | 0.83 d (8.4) |
| 10 | 39.6 | --- |
| 11 | 20.9 | 1.56 m<br>1.67 m |
| 12 | 29.9 | 1.84 t (12.2)<br>2.36 m |
| 13 | 89.6 | --- |
| 14 | 47.1 | 2.17 d (9.8)<br>2.69 d (9.8) |
| 15 | 134.3 | 5.03 s |
| 16 | 144.4 | --- |
| 17 | 12.7 | 1.89 s |
| 18 | 28.0 | 1.35 s |
| 19 | 176.7 | --- |
| 20 | 16.4 | 1.33 s |

7.19 Table 2. $^{1}H$ and $^{13}C$ NMR (500 and 125 MHz, pyridine-$d_5$) Assignments of the CC-00277 C-19 glycoside.

| | CC-00277 | |
|---|---|---|
| Position | $^{13}C$ | $^{1}H$ |
| $Glc_I$-1 | 94.5 | 6.33 d (8.4) |
| $Glc_I$-2 | 76.6 | 4.51 t (8.8) |
| $Glc_I$-3 | 88.3 | 4.99 m |
| $Glc_I$-4 | 69.6 | 4.19 m |
| $Glc_I$-5 | 78.1 | 4.10 m |
| $Glc_I$-6 | 61.5 | 4.21 m<br>4.33 m |
| $Glc_V$-1 | 103.8 | 5.81 d (6.9) |
| $Glc_V$-2 | 75.2 | 4.20 m |
| $Glc_V$-3 | 78.2 | 4.20 m |
| $Glc_V$-4 | 73.1 | 4.10 m |
| $Glc_V$-5 | 77.8 | 3.89 m |
| $Glc_V$-6 | 63.6 | 4.31 m<br>4.62 d (11.1) |
| $Glc_{VI}$-1 | 103.9 | 5.33 d (7.7) |
| $Glc_{VI}$-2 | 75.1 | 3.97 m |
| $Glc_{VI}$-3 | 77.7 | 4.35 t (8.3) |
| $Glc_{VI}$-4 | 70.9 | 4.11 m |
| $Glc_{VI}$-5 | 77.7 | 3.85 m |
| $Glc_{VI}$-6 | 61.8 | 4.12 m<br>4.33 m |

7.20 Table 3. $^{1}H$ and $^{13}C$ NMR (500 and 125 MHz, pyridine-$d_5$) Assignments of the CC-00277 C-13 glycoside.

| | CC-00277 | |
|---|---|---|
| Position | $^{13}C$ | $^{1}H$ |
| $Glc_{II}$-1 | 95.7 | 5.47 d (8.0) |
| $Glc_{II}$-2 | 81.1 | 4.13 m |
| $Glc_{II}$-3 | 87.6 | 4.89 t (8.9) |
| $Glc_{II}$-4 | 70.0 | 4.04 t (8.9) |
| $Glc_{II}$-5 | 77.4 | 3.90 m |
| $Glc_{II}$-6 | 62.4 | 4.17 m<br>4.31 m |
| 6-deoxy-$Glc_{III}$-1 | 104.5 | 5.45 d (7.0) |
| 6-deoxy-$Glc_{III}$-2 | 75.6 | 4.15 m |
| 6-deoxy-$Glc_{III}$-3 | 78.1 | 4.14 m |
| 6-deoxy-$Glc_{III}$-4 | 72.8 | 4.02 m |
| 6-deoxy-$Glc_{III}$-5 | 77.3 | 3.77 m |
| 6-deoxy-$Glc_{III}$-6 | 63.5 | 4.31 m<br>4.53 d (10.9) |
| $Glc_{IV}$-1 | 103.9 | 5.44 d (7.5) |
| $Glc_{IV}$-2 | 75.3 | 3.98 m |
| $Glc_{IV}$-3 | 77.6 | 4.46 t (9.0) |
| $Glc_{IV}$-4 | 71.0 | 4.14 m |
| $Glc_{IV}$-5 | 77.8 | 3.99 m |
| $Glc_{IV}$-6 | 61.8 | 4.12 m<br>4.33 m |